High Performance Computing in plasma physics and magnetic fusion

Eric Sonnendrücker

Max-Planck Institute for Plasma Physics

and

TU Munich

with: Omar Maj, Katharina Kormann, Roman Hatzky, Florian Hindenlang, Emmanuel Franck, Ahmed Ratnani, Yaman Guclu, Natalia Tronko

HPC Days, Lyon, 6-8 April 2016

Outline

Tokamak and stellarator physics
- Turbulence and transport: kinetic
- Large scale instabilities: MHD
- Plasma wave interaction in tokamaks: Maxwell

HPC in the european Fusion community

MHD simulations
- Finite Elements: the Jorek Code
- Efficient DG code for MHD

Gyrokinetic and kinetic models
- Derivation of gyrokinetic model
- From the continuous to the discrete action: FEM-PIC
- Field aligned semi-Lagrangian method
- Efficient 6D Vlasov solvers

Outline

Tokamak and stellarator physics

- Turbulence and transport: kinetic
- Large scale instabilities: MHD
- Plasma wave interaction in tokamaks: Maxwell

HPC in the european Fusion community

MHD simulations

- Finite Elements: the Jorek Code
- Efficient DG code for MHD

Gyrokinetic and kinetic models

- Derivation of gyrokinetic model
- From the continuous to the discrete action: FEM-PIC
- Field aligned semi-Lagrangian method
- Efficient 6D Vlasov solvers

Controlled thermonuclear fusion

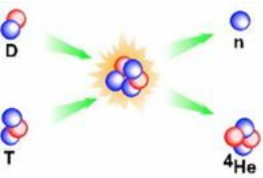

- Fusion conditions:
  $nT\tau_E$ large enough.
- $T \approx 100$ million ^oC
  fully ionized gas=plasma.

- Magnetic confinement (ITER)
- Inertial confinement
  - by laser (LMJ, NIF)
  - by heavy ions

The ITER project

International project involving European Union, China, India, Japan, South Korea, Russia and United States aiming to prove that magnetic fusion is viable source for energy.

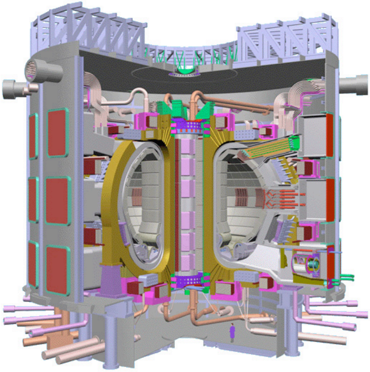

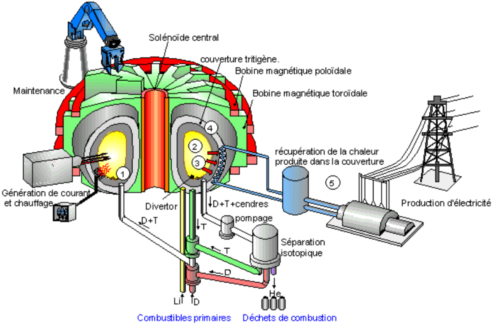

Two devices for magnetic fusion: tokamaks and stellarators

Tokamak

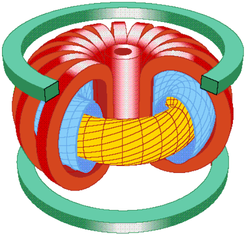

Stellarator

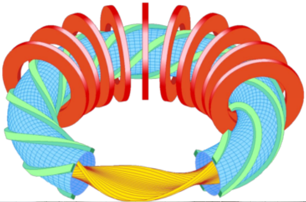

Modelling of Tokamak plasmas

- A plasma is a collection of different species of charged particles.
- Basic model is Newton's law with pairwise interaction between particles which is largely dominated by electromagnetic force. Too many particles $n \approx 10^{19} m^{-3}$, numerically intractable.
- First reduced model: Kinetic Vlasov-Maxwell (+Landau collisions)
- Second reduced model: multi-fluid Euler-Maxwell
- Third reduced model: single fluid MHD
- Other reduced model: Maxwell's equation with dielectric tensor representing plasma

Kinetic models: Turbulent transport

- Plasma not very collisional and far from fluid state
  $\Rightarrow$ Kinetic description necessary for shorter time scales. Fluid and kinetic simulations of turbulent transport yield very different results.
- Vlasov (6D phase space) coupled to 3D Maxwell

$$\frac{\partial f}{\partial t} + \mathbf{v} \cdot \nabla_x f + \frac{q}{m}(\mathbf{E} + \mathbf{v} \times \mathbf{B}) \cdot \nabla_v f = 0.$$

- Toroidal geometry

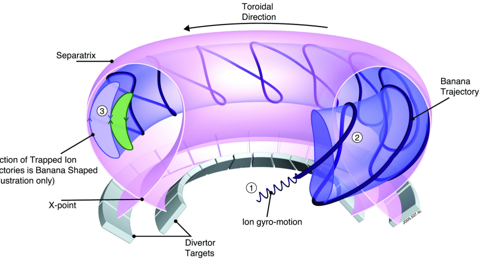

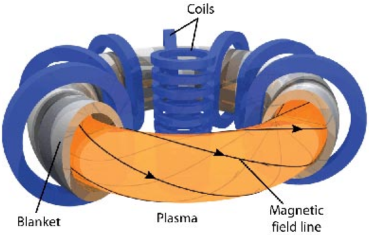

MHD: ELM

- In the tokamak large scale instabilities can appear in the plasma.
- The simulation of these instabilities is an important subject for ITER.

- Example of Instabilities in the tokamak :
  - **Disruptions**: Violent instabilities which can critically damage the Tokamak.
  - **Edge Localized Modes (ELM)**: Periodic edge instabilities which can damage the Tokamak.
- These instabilities are linked to the very large gradient of pressure and very large current at the edge.
- Many aspects of these instabilities are described by fluid models (MHD resistive and diamagnetic or extended)

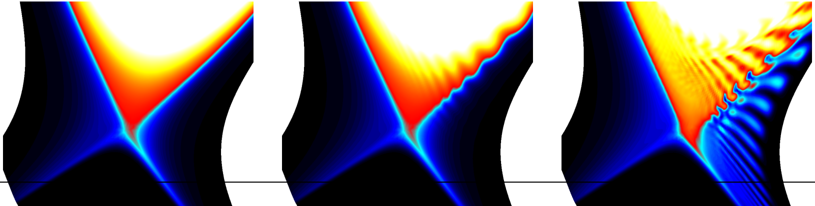

Two-fluid model

- Computing the moments of the Vlasov equation we obtain the following two fluid model

$$
\begin{aligned}
&\partial_t n_s + \nabla_x \cdot (m_s n_s \boldsymbol{u}_s) = 0,\\
&\partial_t (m_s n_s \boldsymbol{u}_s) + \nabla_x \cdot (m_s n_s \boldsymbol{u}_s \otimes \boldsymbol{u}_s) + \nabla_x p_s + \nabla_x \cdot \overline{\overline{\boldsymbol{\Pi}}}_s = \sigma_s \boldsymbol{E} + \boldsymbol{J}_s \times \boldsymbol{B},\\
&\partial_t (m_s n_s \epsilon_s) + \nabla_x \cdot (m_s n_s \boldsymbol{u}_s \epsilon_s + p_s \boldsymbol{u}_s) + \nabla_x \cdot \left(\overline{\overline{\boldsymbol{\Pi}}}_s \cdot \boldsymbol{u}_s + \mathbf{q}_s \right) = \sigma_s \boldsymbol{E} \cdot \boldsymbol{u}_s,
\end{aligned}
$$

- coupled with Maxwell's equations

$$
\frac{1}{c^2} \partial_t \boldsymbol{E} - \nabla \times \boldsymbol{B} = -\mu_0 \boldsymbol{J},
$$

$$
\partial_t \boldsymbol{B} + \nabla \times \boldsymbol{E} = 0,
$$

$$
\nabla \cdot \boldsymbol{B} = 0, \quad \nabla \cdot \boldsymbol{E} = \frac{\sigma}{\varepsilon_0}.
$$

- $n_s = \int_{\mathbb{R}^3} f_s d\mathbf{v}$ the particle number , $m_s n_s \boldsymbol{u}_s = \int_{\mathbb{R}^3} m_s \mathbf{v} f_s d\mathbf{v}$ the momentum, ϵ_s the total energy and $\rho_s = m_s n_s$ the density.
- Isotropic pressures are p_s, stress tensors $\overline{\overline{\boldsymbol{\Pi}}}_s$ and heat fluxes $\mathbf{q}_s$.

MHD: assumptions and generalized Ohm's law

- **quasi neutrality assumption**: $n_i = n_e \Longrightarrow \rho \approx m_i n_i + O(\frac{m_e}{m_i})$, $\mathbf{u} \approx \boldsymbol{u}_i + O(\frac{m_e}{m_i})$
- **Magneto-static assumption** : $\nabla \times \boldsymbol{B} = \mu_0 \boldsymbol{J} + O(\frac{V_0}{c})$.
- We define $\rho = \rho_i + \rho_e$ and $\mathbf{u} = \frac{\rho_i \boldsymbol{u}_i + \rho_e \boldsymbol{u}_e}{\rho}$.
- Consequence of the quasi-neutrality:

$$\boldsymbol{u}_e = \boldsymbol{u} - \frac{m_i}{e\rho}\boldsymbol{J} + O\left(\frac{m_e}{m_i}\right)$$

- Summing the mass and moment equation for the two species we obtain:

$$\partial_t \rho + \nabla \cdot (\rho \boldsymbol{u}) = 0$$

$$\rho \partial_t \boldsymbol{u} + \rho \boldsymbol{u} \cdot \nabla \boldsymbol{u} + \nabla p = \boldsymbol{J} \times \boldsymbol{B} - \nabla \cdot \overline{\overline{\boldsymbol{\Pi}}} + O\left(\frac{m_e}{m_i}\right)$$

- For the pressure equation, we replace the electronic velocity by full velocity using the previous relation.

Extended MHD: model

$$
\begin{aligned}
&\partial_t \rho + \nabla \cdot (\rho \boldsymbol{u}) = 0, \\
&\rho \partial_t \boldsymbol{u} + \rho \boldsymbol{u} \cdot \nabla \boldsymbol{u} + \nabla p = \boldsymbol{J} \times \boldsymbol{B} - \nabla \cdot \overline{\overline{\boldsymbol{\Pi}}},
\end{aligned}
$$

$$
\frac{1}{\gamma - 1} \partial_t p_i + \frac{1}{\gamma - 1} \boldsymbol{u} \cdot \nabla p_i + \frac{\gamma}{\gamma - 1} p_i \nabla \cdot \boldsymbol{u} + \nabla \cdot \mathbf{q}_i = -\overline{\overline{\boldsymbol{\Pi}}}_i : \nabla \boldsymbol{u},
$$

$$
\begin{aligned}
&\frac{1}{\gamma - 1} \partial_t p_e + \frac{1}{\gamma - 1} \boldsymbol{u} \cdot \nabla p_e + \frac{\gamma}{\gamma - 1} p_e \nabla \cdot \boldsymbol{u} + \nabla \cdot \mathbf{q}_e = \frac{1}{\gamma - 1} \frac{m_i}{e\rho} \boldsymbol{J} \cdot \left(\nabla p_e - \gamma p_e \frac{\nabla \rho}{\rho} \right) \\
&- \overline{\overline{\boldsymbol{\Pi}}}_e : \nabla \boldsymbol{u} + \overline{\overline{\boldsymbol{\Pi}}}_e : \nabla \left(\frac{m_i}{e\rho} \boldsymbol{J} \right) + \eta |\boldsymbol{J}|^2,
\end{aligned}
$$

$$
\begin{aligned}
&\partial_t \boldsymbol{B} = -\nabla \times \left(-\boldsymbol{u} \times \boldsymbol{B} + \eta \boldsymbol{J} - \frac{m_i}{\rho e} \nabla \cdot \overline{\overline{\boldsymbol{\Pi}}}_e - \frac{m_i}{\rho e} \nabla p_e + \frac{m_i}{\rho e} (\boldsymbol{J} \times \boldsymbol{B}) \right), \\
&\nabla \cdot \boldsymbol{B} = 0, \quad \nabla \times \boldsymbol{B} = \boldsymbol{J}.
\end{aligned}
$$

- **Remark**: We can write easily the equation on the total pressure $p_e + p_i$. Possible simplification $p_e = p/2$.
- In Black: ideal MHD. In Black and blue: Viscous-resistive MHD. All the terms: Extended MHD.

Microwave beams in plasmas

- RF waves are typically used in magnetic fusion plasmas for
  - Heating: wave energy is transferred to particle motion exploiting the wave-particle resonances in a plasma, selectively heating electrons or ions
  - Current drive: transfer momentum to plasma in order to induce toroidal current to generate poloidal confinement field.
  - Diagnostics: temperature and density of a plasma can be determined by probing the plasma with RF waves
- Standard computations are based on short-wavelength asymptotics (ray tracing, beam tracing, ...).
- Such methods fail in some cases. So called full-wave solvers are then the model of choice.

Full-wave solvers

- Full-wave means Direct numerical solution of Maxwell's equations (including the "full" range of wavelengths).
- Popular approach: Finite Difference Time Domain (Yee's scheme) augmented with one equation for the induced current density J,

$$\begin{cases} \partial_t E - c\nabla \times B + \omega_p F = 0, \\ \partial_t B + c\nabla \times E = 0, \\ \partial_t F - \omega_p E - \omega_c \times F + \nu F = 0, \end{cases} \qquad F = 4\pi J/\omega_p.$$

  (For $\nu = 0$, this is a symmetric hyperbolic system; conserved energy.)
- Does not correctly take into account real geometry.
- New full wave solver based on structure preserving finite elements (FEEC: Arnold-Falk-Winther) under development.

Applications: Beam scattering by turbulence

- Turbulence at the edge of the plasma produces density blobs.
- Time-scale separation: We can consider blobs frozen in time.
- Each blob acts as a defocusing lens that can even split the beam:

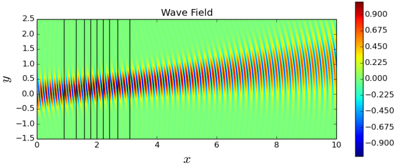

A wave beam injected from the left boundary into a smooth density profile.

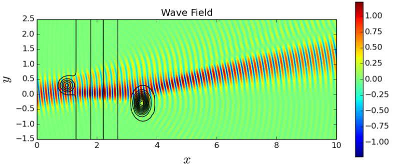

The same beam in presence of two density blobs.

- Standard beam tracing techniques do not apply for such beams.

Applications: Reflectometry diagnostics

- Wave beams are reflected back when the electron density is sufficiently large (cut-off).
- From the phase shift of the reflected beam one obtains information on, e.g., the density profile.
- A fold caustic near the cut-off limits the applicability of ray and beam tracing methods:

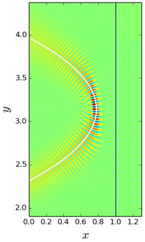

refracted beam
(beam tracing applies)

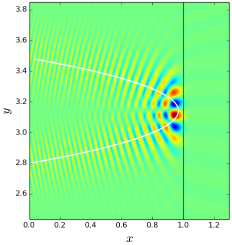

reflected beam
(full-wave required)

Outline

Tokamak and stellarator physics

- Turbulence and transport: kinetic
- Large scale instabilities: MHD
- Plasma wave interaction in tokamaks: Maxwell

HPC in the european Fusion community

MHD simulations

- Finite Elements: the Jorek Code
- Efficient DG code for MHD

Gyrokinetic and kinetic models

- Derivation of gyrokinetic model
- From the continuous to the discrete action: FEM-PIC
- Field aligned semi-Lagrangian method
- Efficient 6D Vlasov solvers

HPC resources

- European Fusion community organised within the EUROfusion consortium supported by EU
- Next to experimental devices HPC plays an important role: dedicated resources
  - HPC-FF (Germany): 2009-2013, 100 Tflops, 1080 nodes, 8-core Intel-Nehalem, 8640 cores. Part of JUROPA cluster at Jülich.
  - HELIOS (Japan): 2012-2016, 1.5 Petaflops, 4500 nodes, 16-core Intel SandyBridge, 72000 cores. Fully dedicated to fusion: 50% for Europe, 50% for Japan.
  - New machine in Italy available at end of this year. Will be part of bigger cluster at CINECA.

The High Level Support Team

- Main tasks for HLST
  The HLST team is a support unit to ensure optimal exploitation of dedicated resources since 2009: HPC-FF, HELIOS, ...
- it is not focused on its own academic research.
- Support for code development
  - Parallelise codes using e.g. OpenMP and/or MPI standards for massively parallel computers
  - Improve the performance of existing parallel codes both at the single node and inter node levels
  - Support the transfer of codes to new multiprocessors architectures
  - Choose and if necessary adapt algorithms and/or mathematical library routines to improve applications for the targeted computer architectures

The NMPP division at IPP

- Numerical Methods in Plasma Physics division at Max-Planck Institute for Plasma Physics
- Develop robust, verified and well-documented codes for plasma physics and magnetic fusion.
- From mathematical modeling to High Performance Computing
- Models derived rigorously from first principles via asymptotic reduction: kinetic, gyrokinetic, fluid, MHD, ...
- Emphasis on well-posedness, energy principle, mathematical structure: basis for verification tests
- Discretisation adapted to features of model: Structure preserving discretisation
- Single core efficiency and parallel scaling important issues.

NMPP code suite

- Well written, tested and documented codes in Fortran 2003
- Can be used for testing new numerical concepts, learning, or as libraries for productions codes. Release versions expected this year.
- Collaborative development under Gitlab at MPCDF
- Major codes:
  - SeLaLib: Kinetic and gyrokinetic, Semi-Lagrangian and PIC (with Inria, U. Strasbourg, CNRS, CEA)
  - Django-Jorek: Finite Element code aimed at MHD (with Inria)
  - Spiga: Finite Element code based on Isogeometric analysis for Maxwell: coupled with particle tracker as a Full Orbit code, Full Wave code in frequency domain under development
  - FEMilaro: Finite Element code for fluid models (SOLPS)

Outline

The JOREK code

- **Models**: reduced MHD models (reduction of the solution space) using potential formulation of the fields.
- **Physics in models**: two fluid and neoclassical effect, coupling with neutral ...
- Typical run of JOREK:
  - Computation of the equilibrium on a grid aligned to the magnetic surfaces.
  - Computation of the MHD instabilities perturbing the axisymmetric equilibrium.

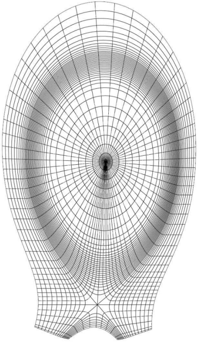

Figure: Aligned grid

Numerical methods

- **Spatial Discretization**: 2D Cubic Bezier finite elements + Fourier expansion.
- **Temporal discretization**: Implicit scheme + Gmres + Toroidal modes Block Jacobi preconditioning

New paths explored for MHD simulations

- JOREK code
  - Verification and non regression tests
  - Scaling issue with present algorithm:
    - Preconditioner for linear system not efficient for strongly non linear problems
    - New preconditioner with better properties has been derived and just being tested
    - Matrix free implementation, where jacobian matrix not explicitly computed, possible. This will overcome the memory limitations.
  - Simplified and modular version of numerical core of JOREK being developed for faster testing and evaluation of numerical algorithms.
- Evaluation of DG code FLEXI from Stuttgart for fusion applications.

Verification of the JOREK model

- The JOREK code implements different variants of reduced resistive MHD. Stability issues observed in some situations.
- A well posed model needs to enforce conservation or dissipation of total energy.
- Original model slightly modified so that the following energy theorem could be proved:

$$\frac{d}{dt}\int_\Omega \left(\frac{|\mathbf{B}|^2}{2} + \rho\frac{|\mathbf{v}|^2}{2} + \frac{1}{\gamma-1}p\right) = -\int_\Omega \eta(T)\frac{|\triangle^*\psi|^2}{R^2} - \int_\Omega \nu|\triangle_\perp u|^2$$

  with $E = \frac{|\mathbf{B}|^2}{2} + \rho\frac{|\mathbf{v}|^2}{2} + \frac{1}{\gamma-1}p$ the total energy,
  $\mathbf{v} = -R\nabla u \times \mathbf{e}_\phi + v_{||}\mathbf{B}$ and ψ the poloidal magnetic flux.
- Modified model has been implemented and indeed remains stable in situations where the original model is not.

Physics Based Preconditioner

- Present JOREK preconditioner based on direct solver for each Fourier mode
- Exact for linear problems, but very inefficient in nonlinear case.
- Stiff problem due to hyperbolic structure with very different wave speeds
- Rewrite the hyperbolic system as a second order equation (well-conditioned): parabolization (L. Chacon).
- First tests on simpler problem exhibiting similar features.
- can be extended to the nonlinear hyperbolic system as MHD (and resistive MHD with additional splitting steps).

Damped waves problem

- We consider the damped wave problem

$$\frac{\partial p}{\partial t} + \frac{1}{\varepsilon}\nabla \cdot \mathbf{u} = 0$$
$$\frac{\partial \mathbf{u}}{\partial t} + \frac{1}{\varepsilon}\nabla p = -\frac{\sigma}{\varepsilon^2}\mathbf{u}$$

  with σ opacity, c light speed and $\varepsilon \approx \frac{1}{c} \approx \frac{1}{\sigma}$
- When $\varepsilon \longrightarrow 0$ the model can be approximated by $\partial_t p - \nabla \cdot (\frac{1}{\sigma}\nabla p) = 0$.
- This problem is stiff in time. CFL condition is $\Delta t \leq C_1 \varepsilon h + C_2 \varepsilon^2$.
  $\Rightarrow$ Use implicit scheme but the model is ill-conditioned
- Two reasons for the ill-conditioning:
  1. the stiff terms (which depend of ε)
  2. the hyperbolic structure.

Results with classical Solvers/Preconditioners

- Comparison between GMRES method with different preconditioning
- Jac (Jacobi), ILU (Incomplete LU), MG (Multigrid), SOR.
- Physics Based (PB)
- $\varepsilon_1 = 10^{-5}$ and $\varepsilon_2 = 10^{-10}$.

Mesh / solvers		Jac	ILU(0)	ILU(4)	MG(2)	SOR	PB
4×4, ε_1	cv	✓	✓	✓	✓	✓	✓
	iter	27	11	1	38	8	1
	time	7.2 E-4	1.3E-3	7.7E-3	1.5E-2	1.4E-3	2.1E-3
4×4, ε_2	cv	✓	✓	✓	✗	✓	✓
	iter	2.1E+4	11	1	-	8	1
	time	3.6E-1	1.3E-3	7.7E-3	-	1.5E-3	2.1E-3
16×16, ε_1	cv	✓	✓	✓	✗	✓	✓
	iter	1.5E+4	18	9	140	20	1
	time	5.0E-0	2.3E-2	4.0E-1	5.0E-1	5.0E-2	2.1E-2
16×16, ε_2	cv	✗	✓	✓	✗	✓	✓
	iter	-	18	9	-	20	1
	time	-	2.3E-2	4.0E-1	-	5.0E-2	2.1E-2
64×64, ε_2	cv	✗	✗	✓	✗	✗	✗
	iter	-	-	632	-	-	1
	time	-	-	2.0E+1	-	-	4.2E-1

Results with the new Preconditioners

- Comparison between GMRES method with different Finite Elements. HB: Cubic Hermite-Bézier, BS(p) splines of degree p at $t = dt$ and $hdt = cst$

Mesh		HB	BS(3)	BS(4)	BS(5)
16×16	cv	✓	✓	✓	✓
	iter	3	2	1	1
	error	2.4E-11	7.7E-16	3.6E-11	1.5E-13
	time	0.38	4.14E-2	1.62E-2	2.1E-2
32×32	cv	✓	✓	✓	✓
	iter	6	2	1	1
	error	3.8E-13	5.8E-14	1.4E-13	5.2E-15
	time	14.08	0.18	5.5E-2	7.28E-2
64×64	cv	✓	✓	✓	✓
	iter	16	1	1	1
	error	4.3E-11	2.3E-12	8.8E-14	1.1E-13
	time	461.1	0.15	0.24	0.44

- The convergence tolerance is 10^{-10} and iter_max=100'000.
- The Preconditioner-solver tolerance is 10^{-7} for convergence and iter_max=1'000.

Comments on new preconditionner

- The good results for B-Splines (with maximum regularity) can be explained by the spectral properties of B-Splines discretized matrices,
- The global time can be improved by deriving appropriate preconditioners or solvers for the subsystems.
- The Generally Locally Toeplitz theory is a very good framework to study and improve the efficiency of a preconditioner
  - $H(\text{div}, \Omega)$ and $H(\text{curl}, \Omega)$ elliptic variational problems (needed for Maxwell, Stokes and some Physics-based subsystems)
  - Fast MultiGrid solver for elliptic problems (does not depend on the degree, nor the domain dimension)

Exploring alternatives for JOREK's fully implicit Finite Elements: the FLEXI DG-SEM code

- FLEXI: Highly scalable explicit 3D DG-SEM solver, high order, unstructured hex-meshes for general conservation laws
- Resistive full MHD & anisotropic diffusion implemented and validated
- Difficulties: Find semi-implicit time integration maintaining scalability of the solver!
- Initialization: domain geometry, mesh and MHD equilibrium needed
- Objectives:
- Assess DG versus JOREK's FE for different fusion applications
- Explore benefits of non conforming locally field aligned mesh which is easier to handle with DG, including in the vicinity of the separatrix.

Discontinuous Galerkin Method

- From high order Finite Element Method (p-FEM):
  Approximation solution is a polynomial inside an element
- From Finite Volume (FV):
  Riemann solvers to resolve discontinuity at element interfaces

⇒ High order scheme, low dissipation and dispersion errors

⇒ Allows coarse unstructured meshes for complex geometries

⇒ High potential for parallel scaling due to element local operators

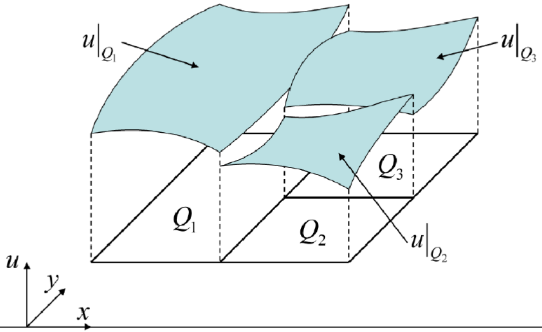

Strong Scaling of FLEXI

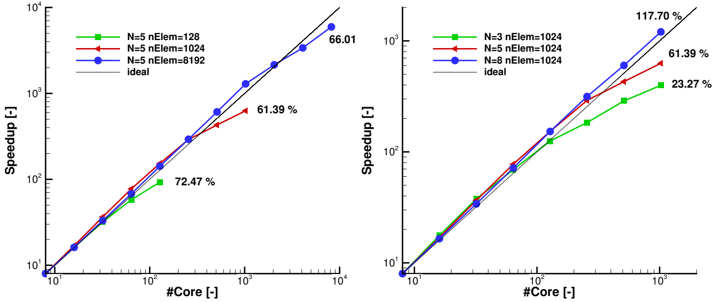

$N = 5$ & different mesh sizes — *$N = 3/5/8$ on same mesh*

- Strong scaling on Cray XE6, HLRS Stuttgart
- Always up to one element per core
- Number of cores is doubled in each step
- Speedup $> 100\%$ owing to cache effects (low memory consumption)

$\Rightarrow$ Ideal strong scaling for ≈ 1000 DOF per core, corresponding to one $N8$-elem., four $N5$-elem. or eight $N3$-elem. per core

High order meshes

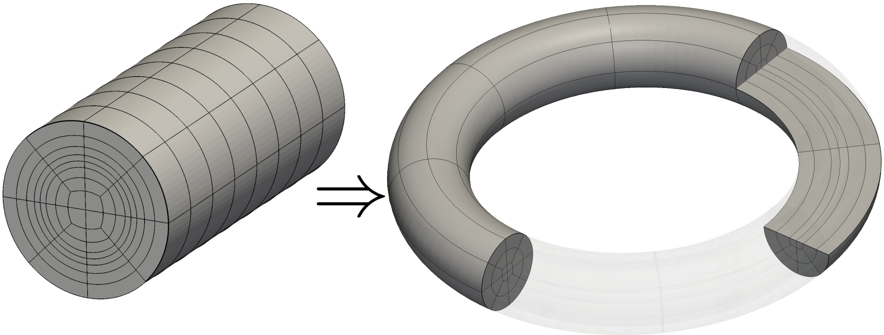

- Block-structured meshes of cylinder (avoid singularity)
- High order polynomial element mappings
- Cylindrical mesh ⇒ mapped to torus

High order meshes

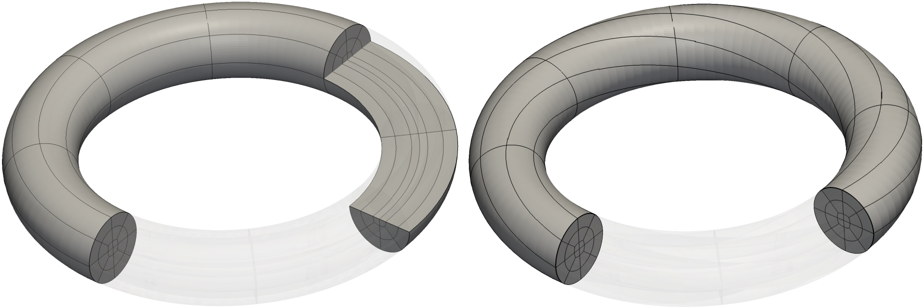

- Mapping approach allows for field alignment in toroidal direction

High order meshes

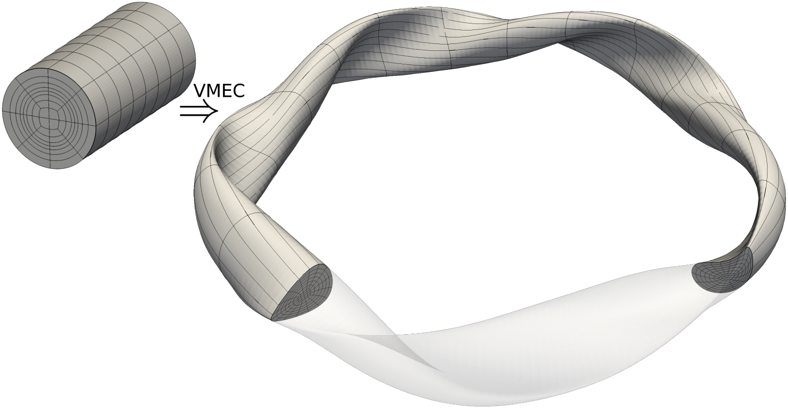

- Interface to VMEC:
  Allows to map Tokamak and Stellarator configurations:

⇒ get mesh geometry & MHD equilibrium [1]

[1] VMEC input provided by C. Nuehrenberg, Greifswald

High order meshes

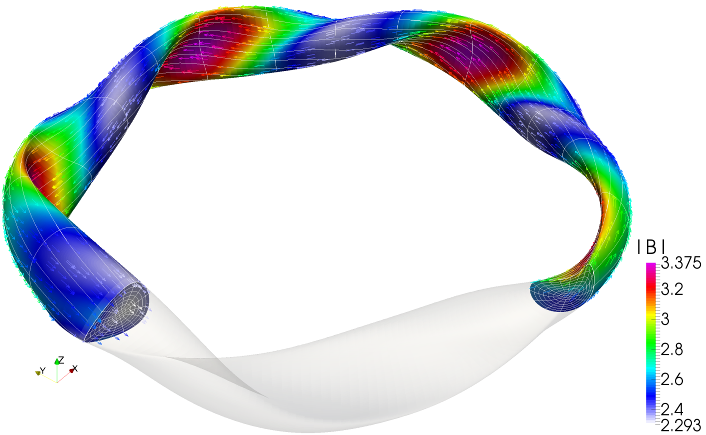

- Interface to VMEC:
  Allows to map Tokamak and Stellarator configurations:

⇒ get mesh geometry & MHD equilibrium [1]

[1] VMEC input provided by C. Nuehrenberg, Greifswald

2D MHD Simulation of a Current Hole Instability

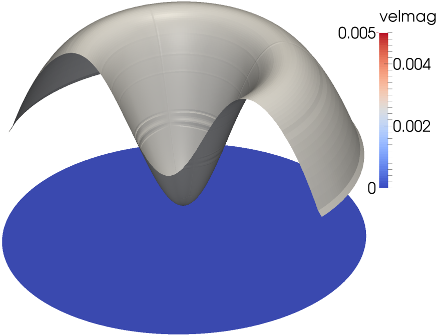

initial current profile

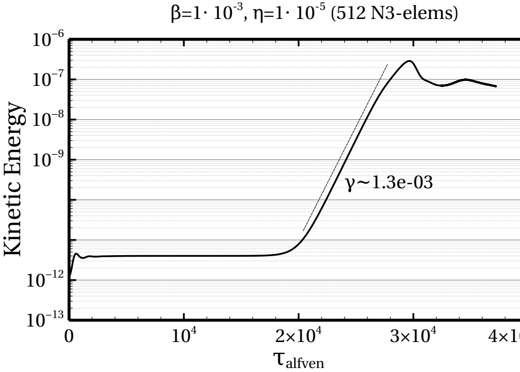

kinetic energy growth

- Cylindrical domain, 512 N3 elements , setup: Czarny and Huysmans[2]
- MHD equilibrium from radial current profile

⇒ Growth rate and solution compares well with reference

[2] O. Czarny,G. Huymans, *Bezier surfaces and FE for MHD simulations*, JCP 226, 2008

2D MHD Simulation of a Current Hole Instability

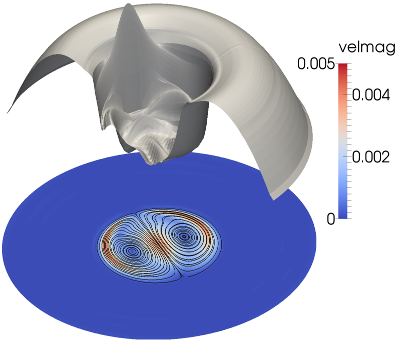

current profile at peak kin. energy

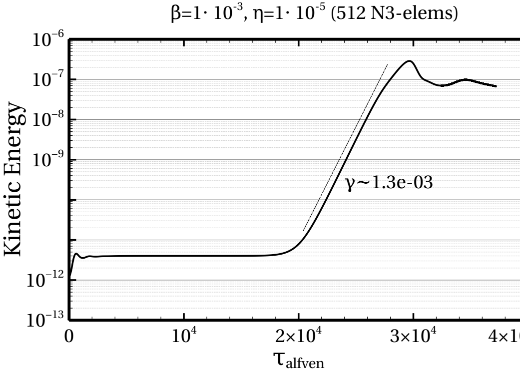

kinetic energy growth

- Cylindrical domain, 512 N3 elements , setup: Czarny and Huysmans[2]
- MHD equilibrium from radial current profile

⇒ Growth rate and solution compares well with reference

[2] O. Czarny, G. Huymans, *Bezier surfaces and FE for MHD simulations*, JCP 226, 2008

Anisotropic diffusion in z-pinch field

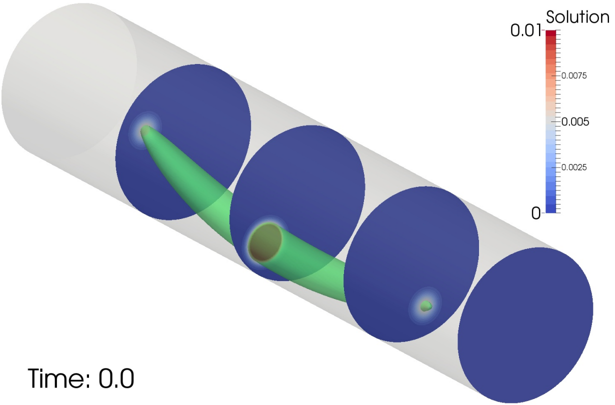

- Diffusion of a blob in Z-pinch magnetic field
- Parallel diff. $\chi_{\parallel} = 1$, perpendicular diff. $\chi_{\perp} = 0$
- Periodic cylindrical domain, 1800 N5 elements

$\Rightarrow$ Field aligned & same accuracy: factor 8 fewer elements!

Anisotropic diffusion in z-pinch field

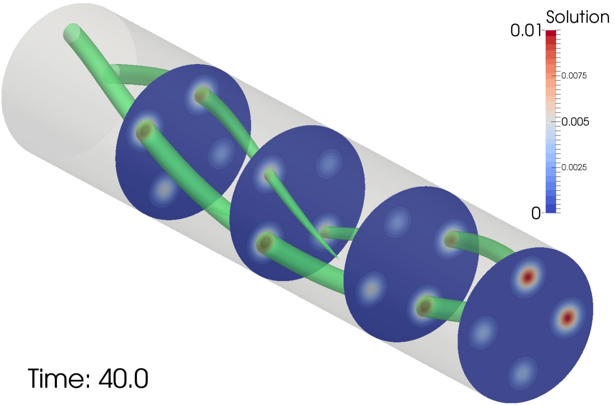

- Diffusion of a blob in Z-pinch magnetic field
- Parallel diff. $\chi_{\parallel} = 1$, perpendicular diff. $\chi_{\perp} = 0$
- Periodic cylindrical domain, 1800 N5 elements

$\Rightarrow$ Field aligned & same accuracy: factor 8 fewer elements!

Anisotropic diffusion in z-pinch field

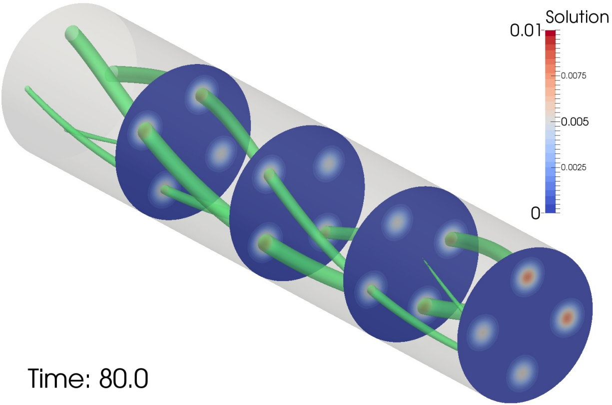

- Diffusion of a blob in Z-pinch magnetic field
- Parallel diff. $\chi_{\parallel} = 1$, perpendicular diff. $\chi_{\perp} = 0$
- Periodic cylindrical domain, 1800 N5 elements

$\Rightarrow$ Field aligned & same accuracy: factor 8 fewer elements!

Anisotropic diffusion in z-pinch field

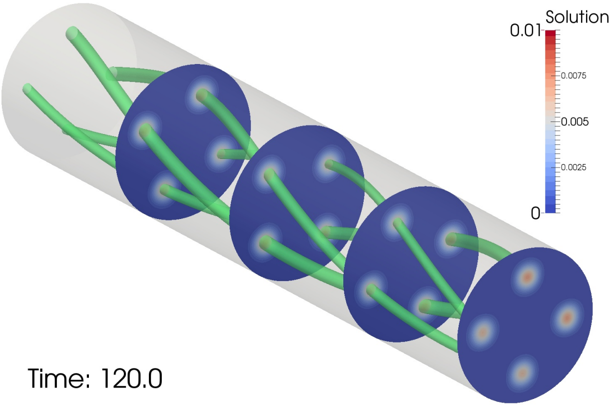

- Diffusion of a blob in Z-pinch magnetic field
- Parallel diff. $\chi_{\|} = 1$, perpendicular diff. $\chi_{\perp} = 0$
- Periodic cylindrical domain, 1800 N5 elements

$\Rightarrow$ Field aligned & same accuracy: factor 8 fewer elements!

Outline

Numerical issues with 6D Vlasov-Maxwell

- Posed in 6D phase space! Dimension reduction if possible would help.
- Large magnetic field imposes very small time step to resolve the rotation of particles along field lines.

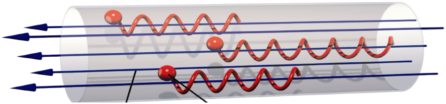

- Physics of interest is low frequency. Remove light waves: Darwin instead of Maxwell.
- Debye length small compared to ion Larmor radius. Quasi-neutrality assumption $n_e = n_i$ needs to be imposed instead of Poisson equation for electric field.

Towards a reduced model

- Scale separation: fast motion around magnetic field lines can be averaged out.
- Idea: separate motion of the guiding centre from rotation by a change of coordinates.
- For constant magnetic field can be done by change of coordinates: $\mathbf{X} = \mathbf{x} - \rho_L$ guiding centre + kind of cylindrical coordinates in $\mathbf{v}$: $v_\parallel$, $\mu = \frac{1}{2}mv_\perp^2/\omega_c$, θ.

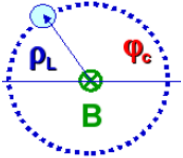

- Mixes position and velocity variables.
- Perturbative model for slowly varying magnetic field.
- Several small parameters
  - gyroperiod, Debye length
  - Magnetic field in tokamak varies slowly: $\epsilon_B = |\nabla B/B|$
  - Time dependent fluctuating fields are small.

Geometric asymptotic reduction

- Long time magnetic confinement of charged particles depends on existence of first adiabatic invariant (Northrop 1963): $\mu = \frac{1}{2} m v_\perp^2 / \omega_c$.
- Geometric reduction based on making this adiabatic invariant an exact invariant.
- Two steps procedure:
  - Start from Vlasov-Maxwell particle Lagrangian and reduce it using Lie transforms such that it is independent of gyromotion up to second order
  - Plug particle Lagrangian into Vlasov-Maxwell field theoretic action and perform further reduction.
- End product is gyrokinetic field theory embodied in Lagrangian. Symmetries of Lagrangian yield exact conservation laws thanks to Noether Theorem.

Historical notes

- Perturbative analysis of Vlasov:
  - linear: Rutherford & Frieman 68, Taylor & Hastie 68, Catto 78
  - non linear: Frieman & Chen 82.
- Hamiltonian methods:
  - electrostatic: Littlejohn 82, 83, Dubin 83
  - Electromagnetic: Brizard, Lee, Hahm 88, Hahm 88
- Gyrokinetic field theory:
  - Lagrangian setting: Sugama 2000, Scott & Smirnov 2010
  - Eulerian setting: Brizard 2000
- Review:
  - Brizard & Hahm 2007
  - Krommes 2012, provides a non technical review of the topic.

Motion of a particle in an electromagnetic field

- Consider given electromagnetic field defined by scalar potential ϕ and vector potential $\mathbf{A}$ such that

$$\mathbf{E} = -\frac{\partial \mathbf{A}}{\partial t} - \nabla\phi, \qquad \mathbf{B} = \nabla \times \mathbf{A}.$$

- The non relativistic equations of motion of a particle in this electromagnetic field is obtained from Lagrangian (here phase space Lagrangian $\mathbf{p}\cdot\dot{\mathbf{q}} - H$ in non canonical variables for later use)

$$L_s(\mathbf{x},\mathbf{v},\dot{\mathbf{x}},t) = (m_s\mathbf{v} + e_s\mathbf{A})\cdot\dot{\mathbf{x}}^2 - (\frac{1}{2}m_s v^2 + e_s\phi).$$

where $\mathbf{p} = m_s\mathbf{v} + e_s\mathbf{A}(t,\mathbf{x})$, $H = m_s v^2/2 + e_s\phi(t,\mathbf{x})$ are canonical momentum and hamiltonian.

Abstract geometric context

- Lagrangian becomes Poincaré-Cartan 1-form

$$\gamma = \mathbf{p} \cdot \mathrm{d}\mathbf{x} - H\,\mathrm{d}t$$

  with $\mathbf{p} = m_s\mathbf{v} + e_s\mathbf{A}(t,\mathbf{x})$, $H = m_s v^2/2 + e_s\phi(t,\mathbf{x})$.
- $\omega = \mathrm{d}\gamma$ is the Lagrange 2-form, which is non degenerate and so a symplectic form. Its components define the the Lagrange tensor Ω.
- Then $J = \Omega^{-1}$ is the Poisson tensor which defines the Poisson bracket

$$\{F, G\} = \nabla F^T J \nabla G$$

- The equations of motion can then be expressed from the Poisson matrix and the hamiltonian

$$\frac{\mathrm{d}\mathbf{Z}}{\mathrm{d}t} = J\nabla H.$$

- Lagrangian contains all necessary information and this structure is preserved by change of coordintates.

Derivation of gyrokinetic particle Lagrangian

- Gyrokinetic particle Lagrangian obtained from Vlasov-Maxwell particle Lagrangian by performing a change of variables, such that lowest order terms independent of gyrophase.
- This is obtained systematically order by order by the Lie transform method (Dragt & Finn 1976, Cary 1981) on the Lagrangian

$$L_s(\mathbf{x}, \mathbf{v}, \dot{\mathbf{x}}, t) = (m_s\mathbf{v} + e_s\mathbf{A}) \cdot \dot{\mathbf{x}}^2 - (\frac{1}{2}m_s|\mathbf{v}|^2 + e_s\phi).$$

- Not a unique solution.
  1. $v_\parallel$ formulation. Transform Lagrangian as is keeping fluctuation **A** in symplectic form.
  2. $p_\parallel$ formulation, $p_\parallel = v_\parallel + (e/m)A_\parallel$. Fluctuating $A_\parallel$ in hamiltonian.
  3. $u_\parallel$ formulation. Split fluctuating $A_\parallel$ into two parts. One of them goes into Hamiltonian. Includes others as special case.
- Gyrokinetic codes choose between $v_\parallel$ (symplectic) and $p_\parallel$ (hamiltonian) formulation.
- Both involve severe numerical drawbacks.

The mixed gyrokinetic particle Lagrangian

- Split $A_\parallel = A_\parallel^s + A_\parallel^h$. Define $u_\parallel = v_\parallel + (e/m)A_\parallel^h$
- The gyrokinetic Lagrangian for a single particle always in the form

$$L = \mathbf{A}^* \cdot \dot{\mathbf{X}} + \mu\dot{\theta} - H$$

$$\text{with } \mathbf{A}^* = \mathbf{A}_0 + \left((m_s/e_s)u_\parallel + \langle A_\parallel^s \rangle\right)\mathbf{b}, \quad \mathbf{b} = \mathbf{B}/B,$$

$$H = H_0 + H_1 + H_2, \quad H_0 = \frac{1}{2}m_s u_\parallel^2 + \mu B, \quad H_1 = \langle \phi - u_\parallel A_\parallel^h \rangle$$

where

$$\langle \psi \rangle(\mathbf{x}, \mu) \stackrel{\text{def}}{=} \frac{1}{2\pi}\oint \psi(\mathbf{x} + \rho)\, \mathrm{d}\alpha.$$

- Perpendicular component of fluctuating vector potential **A** neglected.

The Vlasov equation

- Consider a population of particles evolving with

$$\frac{\mathrm{d}\mathbf{X}}{\mathrm{d}t} = \mathbf{V}, \quad \frac{\mathrm{d}\mathbf{V}}{\mathrm{d}t} = \mathbf{F} = \frac{e}{m}(\mathbf{E} + \mathbf{V} \times \mathbf{B}).$$

- Their distribution function f, or more precisely probability density in phase space (up to normalisation), satisfies the Vlasov equation

$$\frac{\partial f}{\partial t} + \mathbf{v} \cdot \nabla_x f + \mathbf{F} \cdot \nabla_v f = 0.$$

- Given an initial distribution f_0, the distribution at time t is equivalently characterised by the solution of the Vlasov equation or the particle positions $f(t, \mathbf{z}) = f_0(X(0; \mathbf{z}, t), V(0; \mathbf{z}, t))$, where we denote by $\mathbf{z} = (\mathbf{x}, \mathbf{v})$.

Action principle for the Vlasov-Maxwell equations

- Field theory is action principle from which Vlasov-Maxwell equations are derived.
- Action proposed by Low (1958) with a Lagrangian formulation for Vlasov, *i.e.* based on characteristics.
- Based on particle Lagrangian for species s, L_s.
- Such an action, splitting between particle and field Lagrangian, using standard non canonical coordinates, reads:

$$\mathcal{S} = \sum_{\mathrm{s}} \int f_s(\mathbf{z}_0, t_0) L_s(\mathbf{X}(\mathbf{z}_0, t_0; t), \dot{\mathbf{X}}(\mathbf{z}_0, t_0; t), t)\,\mathrm{d}\mathbf{z}_0\,\mathrm{d}t$$

$$+ \frac{\epsilon_0}{2} \int |\nabla \phi + \frac{\partial \mathbf{A}}{\partial t}|^2\,\mathrm{d}\mathbf{x}\,\mathrm{d}t - \frac{1}{2\mu_0} \int |\nabla \times \mathbf{A}|^2\,\mathrm{d}\mathbf{x}\,\mathrm{d}t.$$

Particle distribution functions f_s taken at initial time.

The electromagnetic gyrokinetic field theory

- Gyrokinetics is a low frequency approximation.
  Darwin approximation: $\partial_t \mathbf{A}$ removed from Lagrangian.
- Quasi-neutrality approximation: $|\nabla\phi|^2$ removed:

$$\mathcal{S} = \sum_{\mathrm{s}} \int f_s(\mathbf{z}_0, t_0)(\mathbf{A}^* \cdot \dot{\mathbf{X}} - H)\,\mathrm{d}\mathbf{z}_0 - \frac{1}{2\mu_0}\int |\nabla \times (A_\| \mathbf{b})|^2\,\mathrm{d}\mathbf{x}.$$

- Additional approximation made to avoid fully implicit formulation: Second order term in Lagrangian linearised (consistent with ordering) by replacing full f by background f_M

$$\mathcal{S} = \sum_{\mathrm{s}} \int f_s(\mathbf{z}_0, t_0)(\mathbf{A}^* \cdot \dot{\mathbf{X}} - H_0 - H_1)\,\mathrm{d}\mathbf{z}_0$$
$$- \sum_{\mathrm{s}} \int f_{M,s}(\mathbf{z}_0) H_2\,\mathrm{d}\mathbf{z}_0 - \frac{1}{2\mu_0}\int |\nabla \times (A_\| \mathbf{b})|^2\,\mathrm{d}\mathbf{x}.$$

Derivation of the gyrokinetic equations from the action principle

We denote by $\mathbf{B}^* = \nabla \times \mathbf{A}^*$ and $B_\parallel^* = \mathbf{B}^* \cdot \mathbf{b}$.

- Setting $\frac{\delta \mathcal{S}}{\delta Z_i} = 0$, $i = 1, 2, 3, 4$ yields:

$$\mathbf{B}^* \times \dot{\mathbf{R}} = -\frac{m}{q}\dot{P}_\parallel \mathbf{b} - \frac{1}{q}\nabla(H_0 + H_1), \quad \mathbf{b} \cdot \dot{\mathbf{R}} = \frac{1}{m}\frac{\partial(H_0 + H_1)}{\partial p_\parallel}.$$

- Solving for $\dot{\mathbf{R}}$ and $\dot{P}_\parallel$ we get the equations of motion of the gyrocenters:

$$B_\parallel^* \dot{\mathbf{R}} = \frac{1}{m}\frac{\partial(H_0 + H_1)}{\partial p_\parallel}\mathbf{B}^* - \frac{1}{q}\nabla(H_0 + H_1) \times \mathbf{b}, \; B_\parallel^* \dot{P}_\parallel = -\frac{1}{m}\nabla(H_0 + H_1) \cdot \mathbf{B}^*.$$

- These are the characteristics of the gyrokinetic Vlasov equation

$$\frac{\partial f}{\partial t} + \dot{\mathbf{R}} \cdot \nabla f + \dot{P}_\parallel \frac{\partial f}{\partial p_\parallel} = 0.$$

Gyrokinetic Ampere and Poisson equations

- The gyrokinetic Poisson (or rather quasi-neutrality) equation is obtained by variations with respect to ϕ

$$\int \frac{e_i^2 \rho_i^2 n_{s,0}}{k_\mathrm{B} T_i} \nabla_\perp \phi \cdot \nabla \tilde{\phi} \, \mathrm{d}\mathbf{x} = \int qn \langle \tilde{\phi} \rangle \, \mathrm{d}\mathbf{x}, \quad \forall \tilde{\phi}$$

- The gyrokinetic Ampère equation is obtained by variations with respect to $A_\|$:

$$\int \nabla_\perp A_\| \cdot \nabla_\perp \tilde{A}_\|^h \, \mathrm{d}\mathbf{x} + \sum_s \int \frac{\mu_0 q_s^2 n_s}{m_s} \langle A_\|^h \rangle \langle \tilde{A}_\|^h \rangle \, \mathrm{d}\mathbf{x}$$

$$= \mu_0 \int j_\| \langle \tilde{A}_\|^h \rangle \, \mathrm{d}\mathbf{x}, \quad \forall \tilde{A}_\|^h$$

- where $A_\| = A_\|^s + A_\|^h$ and $A_\|^s$ is related to ϕ by the constraint

$$\frac{\partial A_\|^s}{\partial t} + \nabla \phi \cdot \mathbf{b} = 0.$$

Conserved quantities

- Symmetries of Lagrangian yield invariants using Noether's theorem
- Time translation: Conservation of energy:

$$\mathcal{E}(t) = \sum_s \int \mathrm{d}W_0 \mathrm{d}V_0 f_{s,0}(\mathbf{z}_0) H_s - \int \mathrm{d}V \frac{e_i^2 \rho_i^2 n_{s,0}}{k_\mathrm{B} T_i} |\nabla \phi|^2 + \frac{1}{2\mu_0} \int \mathrm{d}V |\nabla_\perp A_\parallel|^2.$$

- Axisymmetry of background vector potential:
  Conservation of total canonical angular momentum:

$$\mathcal{P}_\varphi = \sum_s e_s \int \mathrm{d}W_0 \mathrm{d}V_0 f_{s,0}(\mathbf{z}_0) \mathbf{A}^\star_{s,\varphi}$$

Discretisation of the action

- Our action principles rely on a Lagrangian (as opposed to Eulerian) formulation of the Vlasov equation: the functionals on which our action depends are the characteristics of the Vlasov equations $\mathbf{X}$ and $\mathbf{V}$ in addition to the scalar and vector potentials ϕ and $\mathbf{A}$.
- A natural discretisation relies on:
  - A Monte-Carlo discretisation of the phase space at the initial time: select randomly some initial positions of the particles.
  - Approximate the continuous function spaces for ϕ and $\mathbf{A}$ by discrete subspaces.
  - Yields a discrete action where a finite (large) number of scalars are varied: the particle phase space positions and coefficients in Finite Element basis.
- When performing the variations, we get the classical Particle In Cell Finite Element Method (PIC-FEM).

FEEC needed for Maxwell's equations

- In order to preserve the continuous structure at the discrete level, the different unknowns ϕ, $\mathbf{A}$, $\mathbf{E}$ and $\mathbf{B}$ need to be chosen in compatible Finite Element spaces.
- This is provided by Finite Element Exterior Calculus (FEEC) introduced by Arnold, Falk and Winther.
- Continuous and discrete complexes are the following

$$
\begin{array}{ccccccc}
H^1(\Omega) & \overset{\textbf{grad}}{\longrightarrow} & H(\textbf{curl},\Omega) & \overset{\textbf{curl}}{\longrightarrow} & H(\mathrm{div},\Omega) & \overset{\mathrm{div}}{\longrightarrow} & L^2(\Omega) \\
\downarrow \Pi_0 & & \downarrow \Pi_1 & & \downarrow \Pi_2 & & \downarrow \Pi_3 \\
V_0 & \longrightarrow & V_1 & \longrightarrow & V_2 & \longrightarrow & V_3
\end{array}
$$

- Faraday and $\mathrm{div}\, B = 0$ verified strongly as

$$
{}^1\mathbf{E} = -\nabla\, {}^0\phi - \frac{\partial\, {}^1\mathbf{A}}{\partial t}, \qquad {}^2\mathbf{B} = \nabla \times\, {}^1\mathbf{A}.
$$

- Ampere and Gauss' law obtained from variations of FE coefficients.

PIC Finite Element approximation of the Action

- Compatible FE discretisation:

$$\phi_h \in V_0, \quad \mathbf{A}_h, \mathbf{E}_h \in V_1, \mathbf{B}_h \in V_2.$$

- Particle discretisation of $f \approx \sum_k w_k \delta(x - x_k(t))\delta(v - v_k(t))$
- Vlasov-Maxwell action becomes:

$$\mathcal{S}_{N,h} = \sum_{k=1}^{N} w_k L_s(\mathbf{Z}(\mathbf{z}_{k,0}, t_0; t), \dot{\mathbf{Z}}(\mathbf{z}_{k,0}, t_0; t), t) - \frac{1}{2} \int |\sum_{i=1}^{N_g} a_i(t) \nabla \times \Lambda_i^1(\mathbf{x})|^2 \, \mathrm{d}\mathbf{x}$$

$$+ \frac{1}{2} \int \left| \sum_{i=1}^{N_g} \phi_i(t) \nabla \Lambda_i^0(\mathbf{x}) + \sum_{i=1}^{N_g} \frac{\mathrm{d}a_i(t)}{\mathrm{d}t} \Lambda_i^1(\mathbf{x}) \right|^2 \, \mathrm{d}\mathbf{x}.$$

- $\mathbf{Z}(\mathbf{z}_{k,0}, t_0; t)$ will be traditionally denoted by $\mathbf{z}_k(t)$ is the phase space position at time t of the particle that was at $\mathbf{z}_{k,0}$ at time t_0.

PIC-FE discretisation of the action

- We know have a discrete action depending on particle positions and Finite Element degrees of freedom, which define the generalised coordinates

$$\mathcal{S}_{N,h}[\mathbf{x}_1, \ldots, \mathbf{x}_N, \dot{\mathbf{x}}_1, \ldots, \dot{\mathbf{x}}_N, \mathbf{v}_1, \ldots, \mathbf{v}_N, \phi_1, \ldots, \phi_{N_g}, a_1, \ldots, a_{N_g}]$$

- The discrete electric and magnetic fields are defined exactly as in the continuous case from the discrete potentials thanks to the compatible Finite Element spaces

$$\mathbf{E}_h = \sum_i e_i \Lambda_i^1(\mathbf{x}) = -\nabla \phi_h - \frac{\partial \mathbf{A}_h}{\partial t}, \quad \mathbf{B}_h = \sum b_i \Lambda_i^2(\mathbf{x}) = \nabla \times \mathbf{A}_h.$$

- It immediately follows like in the continuous case the discrete Faraday equation

$$\frac{\partial \mathbf{B}_h}{\partial t} + \nabla \times \mathbf{E}_h = 0.$$

Time advance via Hamiltonian splitting

- Following the prescription of Crouseilles-Einkemmer-Faou a Hamiltonian splitting can be performed, treating the three terms of the Hamiltonian separately

$$H = \frac{1}{2}\mathbf{v}M_p\mathbf{v} + \frac{1}{2}\mathbf{e}M_1\mathbf{e} + \frac{1}{2}\mathbf{b}M_2\mathbf{b} = H_p + H_e + H_b.$$

- Split and solve successively ($\Omega(u)$ Poisson matrix)

$$\frac{\mathrm{d}u}{\mathrm{d}t} = \Omega(u)\nabla H_i, \quad i = p, e, b$$

- Lie-Trotter splitting (first order), Strang splitting (second order) or even higher order.
- Exact solution possible for H_e and H_b.
- For H_p split further between the three components. Other possibility: use variational integrator

Comments and related work

- Variational FE-PIC codes along with control variates for noise reduction at the base of success of PIC simulations of Tokamak turbulence with ORB5 family of codes.

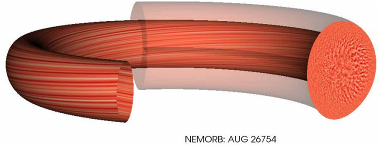

(Picture: A. Bottino)

- A lot of recent effort towards variational or Hamiltonian discretisation of Vlasov (or related)
  - First ref: Lewis, Energy conserving numerical approximations of Vlasov plasmas, JCP 1970
  - Shadwick, Stamm, Estatiev, Variational formulation of macro-particle plasma simulation algorithms (Phys Plasmas 2014)
  - Squire, Qin, Tang, Geometric integration of the Vlasov-Maxwell system with a variational particle-in-cell scheme, (Phys Plasmas 2012)

Hierarchy of nonlinear Gyrokinetic Maxwell-Vlasov models for verification of global GK codes

- European project VeriGyro:
  - Most popular tools for plasma turbulence investigation
  - Extended development over last 10 years
  - Variety of implemented GK models
- Building up hierarchy of Gyrokinetic models implemented into the codes:
  - Systematic derivation from the Variational GK framework
  - Verification of approximations consistency
  - Identification of regimes of applicability
- Intercode Benchmark: implicit numerical schemes verification
  - Hierarchy of numerical test cases: from adiabatic electrons towards linear electromagnetic simulation.
  - Participating codes: GENE/GKW (Eulerian); ORB5/EUTERPE (PIC); GYSELA (Semi - Lagrangian)

Linear electromagnetic benchmark

- Second order Gyrokinetic theory for Particle-In-Cell code ORB5
- Intercode linear electromagnetic Benchmark (ORB5 & GENE)
- Identification of instabilities transitions: from ITG (low frequencies) to KBM (high frequencies)

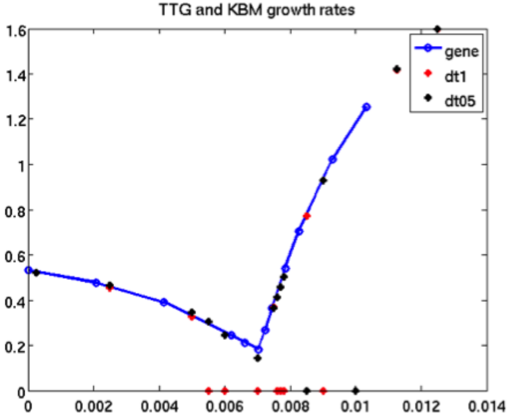

Gyrokinetics: field-aligned semi-Lagrangian schemes

Ultimate Goals

- Gyrokinetics: non-linear, electromagnetic, with multiple species
- Complex 3D geometries (Tokamaks and Stellarators)
- Global simulations (including magnetic axis and X point)

Opposing Requirements

- **Efficiency**: minimize number of degrees of freedom
- **Geometry**: flexible and robust 3D meshing, e.g. mapped multiblock grids (see figure)

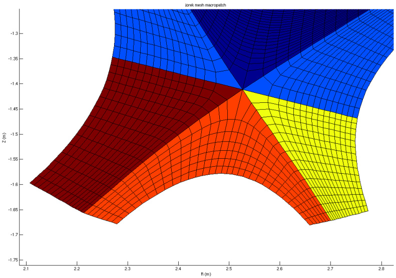

Gyrokinetics: field-aligned semi-Lagrangian schemes

Observation

- Linear instability modes have large parallel wavelengths ($\lambda_\parallel \gg r_{Li}$)
- Turbulence structures also have small parallel gradients ($\nabla_\parallel \ll \nabla_\perp$)

Magnetic flux coordinates

- Allow for great reduction of grid points along one direction
- Shortcomings: singularities (magnetic axis, X-point), complex meshing, inhomogenous grid spacing

Field-aligned approach

- Allows reduction of grid points along toroidal direction φ
- Great mesh flexibility, uses interpolation on poloidal plane

Gyrokinetics: field-aligned semi-Lagrangian schemes

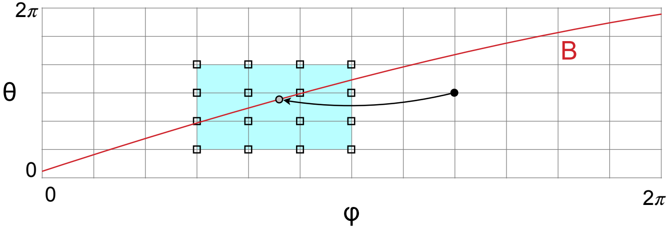

Standard Interpolation

- centered rectangular stencil
- requires fine mesh in φ

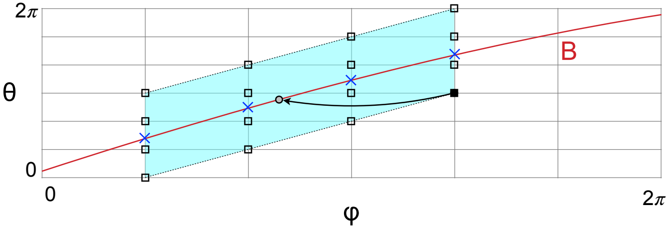

Field-Aligned Interpolation

- stencil adapts to magnetic field line
- allows for coarser mesh in φ

Gyrokinetics: field-aligned semi-Lagrangian schemes

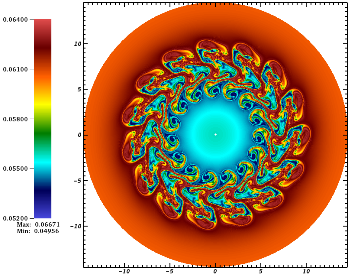

Progress in SeLaLib

- ITG instability in screw-pinch geometry
- Uniform mesh in polar coordinates
- Verification: growth rates match analytics
- Figure: distribution function at $\varphi = 0$, $v_{\|} = 0$

	Geometry	Equations
Current State	theta-pinch screw-pinch cylindrical Tokamak (in Gysela)	gyrokinetic ($\mu = 0$) ions adiabatic electrons electrostatic limit
Next Steps	bumpy-pinch (straight stellar.) Tokamak (Asdex-U, ITER) Stellarator (Wendelstein 7-X)	fully gyrokinetic ions gyrokinetic ($\mu = 0$) electrons electromagnetic

Vlasov equation in 6D

Goal:

- Develop efficient semi-Lagrangian solver of Vlasov equation in 6D
- Study physical problems to verify/improve gyrokinetics

First test case: Simulation of ITG in slab with periodic boundary conditions

Verification: Comparison to dispersion relation

- frequency: dispersion $\omega_r \approx -0.01854$, simulated $\omega_r \approx -0.0185$
- growth rate: see figure

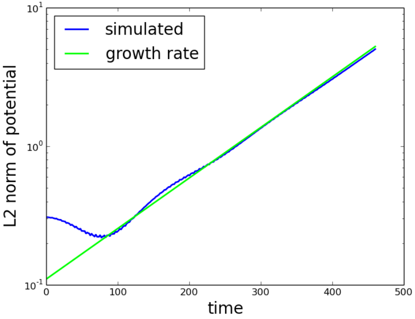

Efficient parallelization strategies for 6D Vlasov

Two approaches:

- Remap: Work with two domain partitions, one keeping the spatial coordinates local and one keeping the velocity coordinates local $\rightsquigarrow$ transpose of data in all-to-all communication.
- Domain decomposition (DD): Work with one domain partitioning which consists of 6D subblocks of the total data $\rightsquigarrow$ neighbor-neighbor communication.

Results:

- Data exchange dominates.
- Lagrange interpolation better suited for DD than splines.
- DD allows for optimizations by exchange of data in 32-bit and compression.

6D Vlasov solver on sparse grids

Idea of sparse grids: Down-sampling of full grid to reduce the curse of dimensionality in an optimal way for a given class of functions.

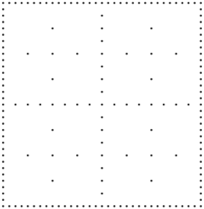

from: Garcke, Sparse grid tutorial

Key features of the solver:

- Representation of the distribution function on tensor product of sparse grids in x and v.
- Propagation with semi-Lagrangian method: Combine sparse-grid interpolation with 1D spline interpolation.
- Multiplicative δf-method: Only a (multiplicative) deviation from an equilibrium state is represented on the sparse grid.

6D Vlasov solver on sparse grids

Results:

- Good compression can be achieved if close to equilibrium
- Numerical instabilities can occur if problem is severely underresolved

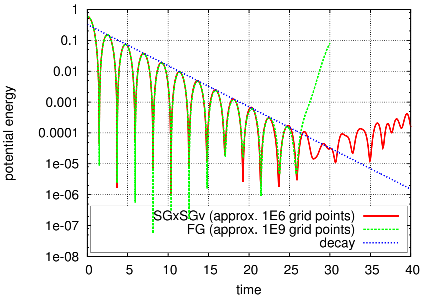

Next steps:

- Improve parallelization stategy for 6D solver.
- Consider configurations with magnetic fields with sparse grid or low-parametric tensor solver.

Tensor train representation

- Very efficient solver with optimal complexity ($O(N)$ or $O(N \log_2 N)$) has been developed for 6D Vlasov-Poisson equations.
- However 6D grid is huge: e.g. $N = 64^6 \approx 70 \times 10^9$.
- Idea: Use low-rank tensor representation

$$Q(x_1, \dots, x_d) = \sum_{\alpha_1, \dots, \alpha_{d-1}} Q_1(x_1, \alpha_1) Q_2(\alpha_1, x_2, \alpha_2) \dots Q_d(\alpha_{d-1}, x_d)$$

to represent the data more efficiently.

- Semi-Lagrangian method developed within the Tensor Train framework.
- Result: Data compression but more complex algorithms (QR and SVD of the kernels to recompress data).

Prototype MATLAB implementation

- Nonlinear Landau damping problem.
  Computing time (wall clock time) and memory of a tensor representation (TT) compared to the solution on the full grid (FG) for 1146 iterations.

dim	method	# doubles for f	fraction	wall time	fraction
2D	FG	4096		$1.5 \cdot 10^{1}$	
2D	TT	2720	0.66	$6.8 \cdot 10^{0}$	0.45
4D	FG	$1.7 \cdot 10^{7}$		$6.2 \cdot 10^{4}$	
4D	TT	$5.5 \cdot 10^{4}$	$3.3 \cdot 10^{-3}$	$6.0 \cdot 10^{2}$	$9.7 \cdot 10^{-3}$
6D	TT	$3.1 \cdot 10^{6}$	$4.5 \cdot 10^{-5}$	$2.7 \cdot 10^{4}$	

Next steps

- High-performance implementation based on efficient dense linear algebra packages.
- Solution of Vlasov–Maxwell equations.

Conclusions and perspectives

- Applied math and HPC a strong need of magnetic fusion research
- Very complex models. Solid theory and verification strategy required.
- Gyrokinetic and kinetic simulations posed in 5D or 6D phase space require a lot of resources and scale well with some effort.
- Verification and development based on modern software engineering concepts needed.